

Supplementary Information

CdSe/CdS-Quantum Rods: Fluorescent Probes for *in vivo* Two-Photon Laser Scanning Microscopy

Jelena Dimitrijevic^{a‡}, Lisa Krapf[‡], Christopher Wolter^{a‡}, Christian Schmidtke^a, Jan-Philip Merkl^a, Tobias Jochum^b, Andreas Kornowski^a, Anna Schüth^d, Andreas Gebert^d, Gereon Hüttmann^c, Tobias Vossmeier^{a}, and Horst Weller^{a,b,e,f*}*

^a Institute of Physical Chemistry, University of Hamburg, Grindelallee 117, 20146 Hamburg, Germany.

* E-mail: tobias.vossmeier@chemie.uni-hamburg.de; horst.weller@chemie.uni-hamburg.de

^b Centrum für Angewandte Nanotechnologie (CAN) GmbH
Grindelallee 117, 20146 Hamburg (Germany).

^c Institute of Biomedical Optics, University of Lübeck
Peter-Monnik-Weg 4, 23562 Lübeck, (Germany).

^d Institute of Anatomy, University of Lübeck
Ratzeburger Allee 160, 23538 Lübeck (Germany).

^e The Hamburg Centre for Ultrafast Imaging, Luruper Chaussee 149, 22761 Hamburg, Germany

^f Department of Chemistry, Faculty of Science, King Abdulaziz University, Jeddah, Saudi Arabia
current address of AS:

Department of Urology, School for Mental Health and Neuroscience, Maastricht University
Universiteitssingel 40, P.O. Box 616, 6200 MD Maastricht (The Netherlands).

current address AG:

Institute of Anatomy II, University Hospital Jena
Teichgraben 7, 07740 Jena (Germany).

[‡] These authors contributed equally to this paper.

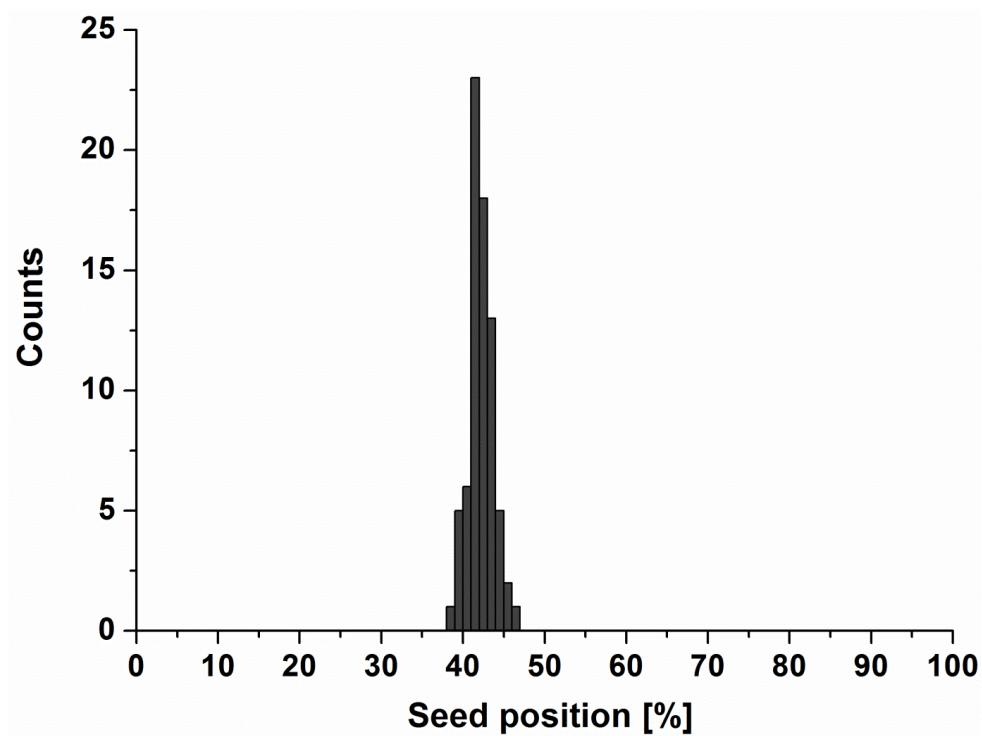


Figure S1. Statistical evaluation of the CdSe-core position within the CdS-rod. The CdSe-core positions were determined by EFTEM measurements of sulfur $L_{2/3}$.

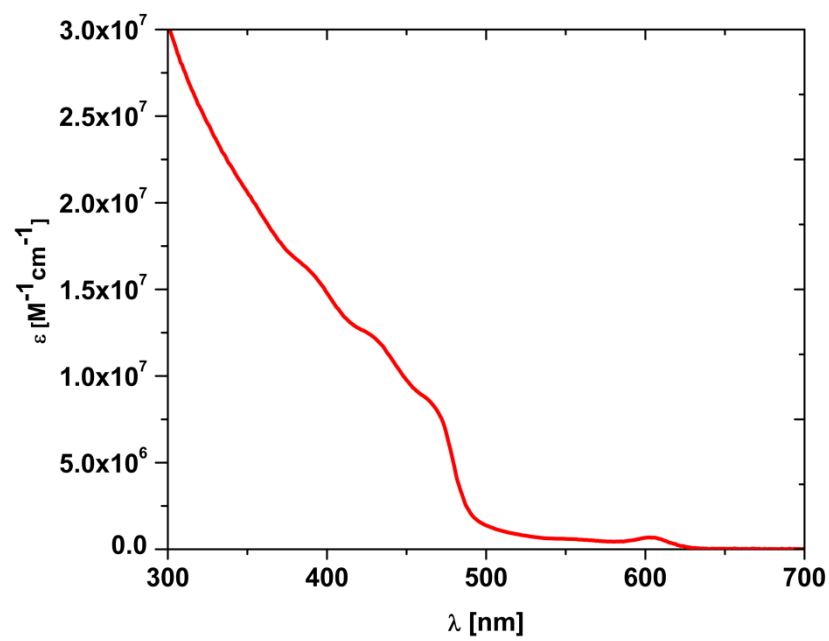


Figure S2. Molar extinction coefficient of investigated CdSe/CdS QDQRs.

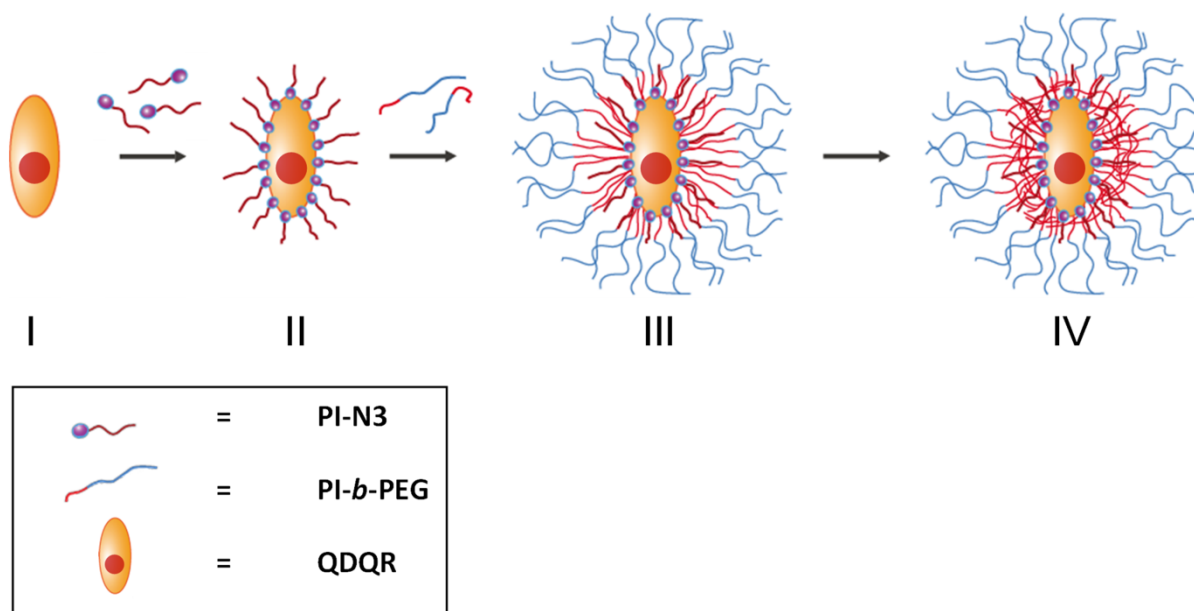


Figure S3. For the phase transfer into aqueous solution the ligands of the as-synthesized QDQRs (e.g. TOP, TOPO) were exchanged by PI-N3 in organic solution. After this, the rods were encapsulated by amphiphilic PI-*b*-PEG ligands with the hydrophobic PI-block interlacing the PI-ligands on the nanorod surface. The organic mixture was injected into aqueous solution to form a dispersion of PI-*b*-PEG-encapsulated QDQRs. The intermediate PI-shell was crosslinked using AIBN as radical initiator.

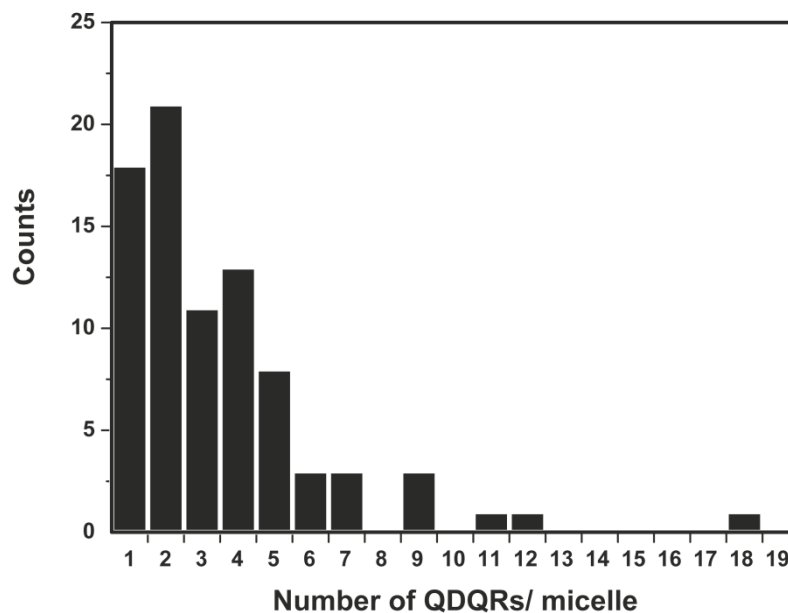


Figure S4. Statistical evaluation of the number of QDQRs per micelle.

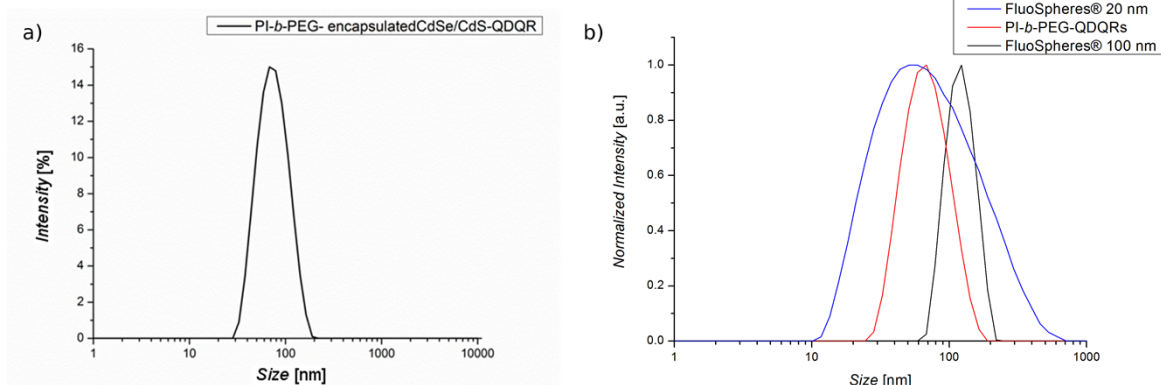


Figure S5. **a)** Size distribution of PI-*b*-PEG-encapsulated QDQRs in water determined by dynamic light scattering. The size distribution did not change significantly over a period of 3 months. **b)** Size distribution of PI-*b*-PEG-encapsulated QDQRs (sample B) and commercially available dye loaded polystyrene beads (FluoSpheres®) with nominal diameters of 20 nm and 100 nm (as given by the supplier) in water determined by dynamic light scattering.

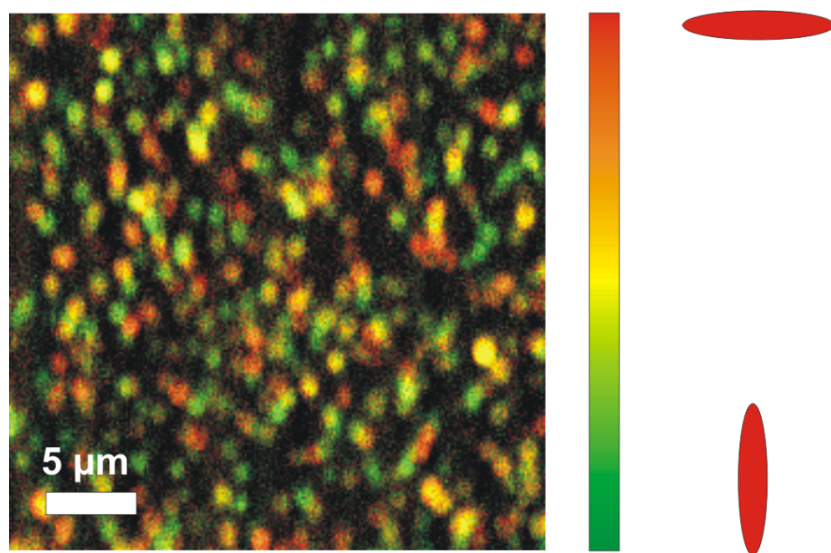


Figure S6. Polarized photo luminescence from QDQRs. Fluorescence was separated in two perpendicularly orientated polarizations by a polarizing beamsplitter. Two PMTs with additional polarizing filters were used to detect parallel and perpendicular orientated fluorescence radiation from single QDQRs or small aggregates. Green color represents vertical orientation, red color represents horizontal polarization, as indicated on the right hand side of the micrograph.

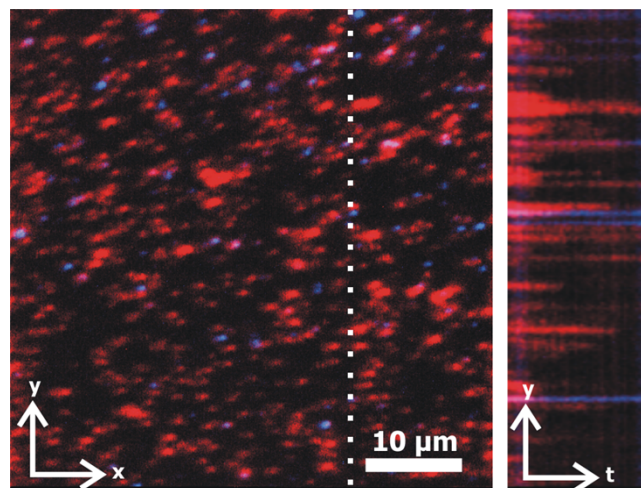


Figure S7. TPLSM image of PI-*b*-PEG encapsulated QDQRs together with FluoSpheres®. The left part shows the PI-*b*-PEG-encapsulated QDQRs (sample B, red color) together with FluoSpheres® (~120 nm DLS size) (blue color) under comparable conditions to the in vivo TPLSM experiment. The right part of the figure shows the fluorescence intensity recorded at the position of the dashed line while imaging the sample for 1 hour.

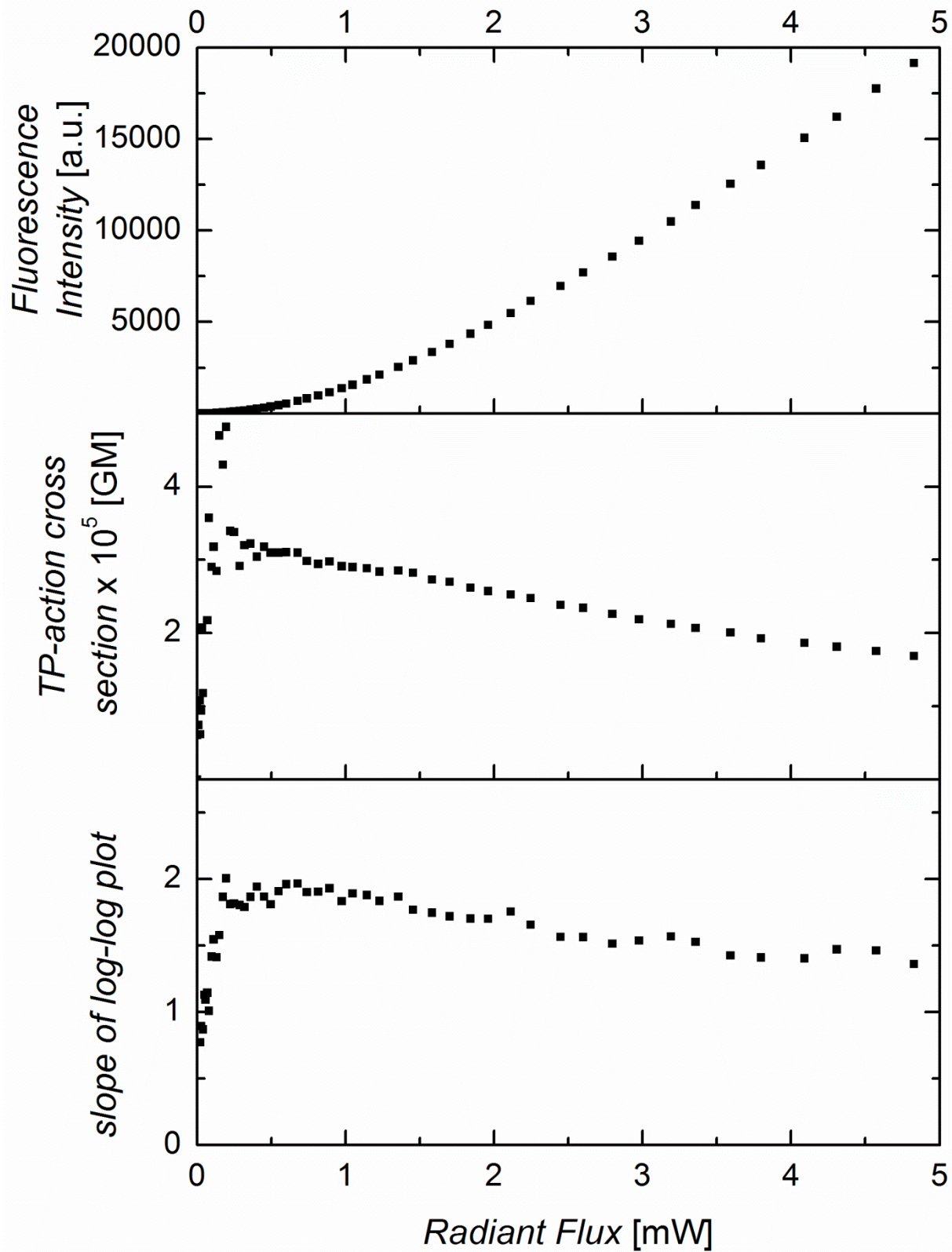


Figure S8. PL-intensity vs. laser power, TP-action cross section vs. laser power, slope of a log-log plot of emission intensity vs. excitation power.